Exploring the Potential of Whey Ultrafiltration Permeate in Wood Modification: Changes in Wood Hygroscopic and Thermal Behaviors

Assira Keralta , ^a Jérémy Winninger, ^a Julien Chamberland , ^b and Véronic Landry , ^a,*

Wood's hygroscopic nature limits its outdoor applications. Technologies such as wood polyesterification, involving the in situ reaction of alcohols and carboxylic acids, densify the wood cell wall and potentially reduce hydroxyl group activity. Whey ultrafiltration permeate, a co-product of whey protein purification, which is rich in lactose, can be a source of OH groups for wood modification. This study explores lactose's reactivity with biobased carboxylic acids and evaluates the resulting wood properties post-modification. Spectroscopic analyses confirmed that lactose reacts with carboxylic acids when heated above the melting point, and the Maillard reaction and caramelization may occur due to whey ultrafiltration permeate's non-protein nitrogen substances and acidic medium combined with high temperatures. Fourier Transform infrared spectroscopy analysis verified that lactose and malic acid react within trembling aspen sawdust, significantly reducing moisture absorption and enhancing thermal stability. This study proposes a novel valorization of whey ultrafiltration permeate and a simple process for improving wood properties.

DOI: 10.15376/biores.20.3.5843-5869

Keywords: Whey ultrafiltration permeate; Lactose; Biosourced acids; Solid-state polycondensation; Wood hygroscopicity; Wood modification

Contact information: a: Department of Wood and Forest Sciences, Renewable Materials Research Center, Université Laval, 2425 Rue de la Terrasse, Quebec City, Canada, G1V 0A6; b: STELA Dairy Research Center, Institute of Nutrition and Functional Foods (INAF), Department of Food Science, Université Laval, 2425 Rue de l'Agriculture, Quebec City, Canada, G1V 0A6;

INTRODUCTION

Wood is a natural composite that is valued for its high physical strength, ease of machining, aesthetic appeal, and abundant supply as a renewable and biodegradable resource. It has a long-standing history of utilization across various industries, particularly in construction and furniture manufacturing. However, its low dimensional stability with humidity changes and its poor resistance to microorganisms, both explained by its hygroscopicity, have posed challenges to its widespread application. Wood's capacity to absorb and release moisture induces dimensional changes until it reaches the fiber saturation point, corresponding to a wood moisture content of approximately 30% in wood. Studies have also shown that microorganisms are larger than the pores of the wood cell wall, thus preventing them from penetrating it (Srebotnik *et al.* 1988; Hill 2002; Hill *et al.* 2005). However, the dimensional variations of the wood create deformations, cracks, and fissures, opening doors for microorganisms to penetrate and degrade the wood. Hill (2002)

^{*} Corresponding author: assira.keralta.1@.ulaval.ca

demonstrated that reducing the amount of moisture in wood leads to decreased diffusion coefficients for the transport of substances in the cell wall, inhibiting the ingress of diffusible agents from fungi. Increasing the dimensional stability of wood and its resistance to microorganisms, therefore, comes down to reducing the wood's hygroscopicity (Hill 2006). There are two sites in wood responsible for moisture absorption (Popescu *et al.* 2014). The free OH groups in cellulose chains (mostly in the amorphous region) and hemicellulose are identified as the primary sites of moisture absorption. The void volume in wood is considered as the second site for moisture absorption. Trapping or eliminating these sites reduces the wood's hygroscopicity. As such, wood stabilization technologies aim to eliminate or trap the free OH groups or fill the voids in the wood.

Wood thermal treatment, acetylation, furfurylation, and polyesterification are among the methods developed for stabilizing wood over the years. Nowadays, there is a growing demand for non-toxic products derived from renewable resources that remain stable in wood and do not release toxic substances during the wood material's service life. This has generated significant interest in modifying wood through polyesterification (Hill 2011). Wood polyesterification involves impregnating wood with a carboxylic acid and an alcohol (source of OH groups) and heating it to carry out esterification (Halpern *et al.* 2014; Berube *et al.* 2018; Kurkowiak *et al.* 2023). This process leads to the formation of polyesters, which densify the cell walls and trap moisture absorption sites. Figure 1 presents the esterification reaction that produces water, which, if not eliminated, can make this reaction reversible through hydrolysis. This reaction performs optimally in a dry or non-aqueous medium. Grosse *et al.* (2018) demonstrated that treating beech wood (*Fagus sylvatica* L.) with lactic acid through polyesterification results in significantly improved dimensional stability and resistance to biological degradation when compared to untreated beech wood (Grosse *et al.* 2018).

$$R \longrightarrow 0$$
 $+$ $HO \longrightarrow R_1$ $=$ 1 $R \longrightarrow 0$ $+$ H_2O

Acid Alcohol Ester

Fig. 1. Esterification (1) and hydrolysis (2) reactions

The utilization of biosourced polymers and by-products from the agricultural and food industries has gained considerable attention in recent years. These materials offer the dual advantage of valorizing waste streams and providing environmentally friendly solutions for various applications. One such innovative approach is using whey ultrafiltration permeate (used as WUFP for Tables and Figures), a co-product of dairy processing, as a potential agent for wood stabilization. Whey ultrafiltration permeate contains lactose (approximately 5% w/w), non-protein nitrogenous compounds (less than 0.5% w/w, including molecules such as urea or amino acids), and minerals (less than 0.5% w/w). It is abundantly generated in North America and is still considered an effluent in many processing plants. In 2022, the United States produced 559,000 metric tons of whey ultrafiltration permeate, a 4.5% increase from the previous year, accounting for 56% of global production of whey ultrafiltration permeate (Source: USDEC and industry estimates).

Whey ultrafiltration permeate is a diluted fluid containing around 5% of solids (Chamberland *et al.* 2020). Due to its lactose content, whey ultrafiltration permeate has a chemical oxygen demand (COD) and biochemical oxygen demand (BOD) of 56,000 and 29,000 mg/L (Chamberland *et al.* 2020), respectively. Thus, direct discharge in nature is not permitted. Whey ultrafiltration permeate is mainly processed to make a powder called deproteinized whey powder, which is commonly used in human or animal nutrition. Due to its low solid content, upcycling strategies generally require energy-intensive processes, making them more expensive than disposal costs, notably when permeate must be transported.

Wood modification using whey ultrafiltration permeate involves an esterification reaction between the lactose contained in whey ultrafiltration permeate and an acid. Lactose has eight hydroxyl groups in its structure, allowing it to react with a carboxylic acid to form an ester when sufficient heat is applied. Although lactose is a hydrophilic molecule, its reaction with citric acid changes its nature. The modified lactose thus becomes hydrophobic. This last property is of great interest for wood during its modification to decrease its hygroscopicity. In a previous study, Cadieux-Lynch *et al.* (2024) demonstrated that the lactose in whey ultrafiltration permeate can react with citric acid when cured at 160 °C for 24 h. They also showed that this reaction can occur within the wood structure of trembling aspen (*Populus tremuloides* Michx.) and black spruce (*Picea mariana*). The resulting products form mainly in the wood cell wall, increasing the wood's dimensional stability by 54% and 49% for trembling aspen and black spruce, respectively (Cadieux-Lynch *et al.* 2024).

The objective of this study was to optimize the innovative lactose-based wood treatment developed previously by Cadieux-Lynch *et al.* (2024). This article is divided in three parts. It presents an investigation of the effect of pH on the thermal degradation of the whey ultrafiltration permeate and pure lactose. Secondly, it compares the efficiency of different biosourced carboxylic acids (citric, fumaric, malic, and succinic) to esterify, in a solid-state reaction, lactose (pure or in whey ultrafiltration permeate powder). Finally, it determines the effectiveness of whey ultrafiltration permeate and the most promising acid (malic acid) in enhancing the chemical, hygroscopic as well as thermal properties of trembling aspen (*Populus tremuloides*) sawdust.

EXPERIMENTAL

Materials

Citric acid (CA) ≥99.5%, fumaric acid (FA) ≥99.0%, malic acid (MA) ≥99.5%, and high-purity succinic acid (SA) were purchased from Sigma Aldrich (Oakville, Canada) and used as received. These acids were selected due to their biobased and multifunctional nature. Their varying physical and chemical characteristics, as detailed in Table 2, offer a better insight into the properties that impact polyesterification and side reactions. Whey ultrafiltration permeate and lactose (>99.0%) powders were provided by Agropur (Longueuil, QC, Canada). Whey ultrafiltration permeate (refers as whey UF permeate in Tables and Figures) contained 88% lactose, 5.8% ash, 2% non-protein nitrogen on a dry basis, and 4% w/w moisture. Trembling aspen (*Populus tremuloides*) sawdust was prepared by screening solid wood pieces with a 30-mesh sieve. The sawdust was stored in a conditioning room (21°C, 41% RH) before treatment.

Thermal Degradation of Permeate Powder and Lactose

The thermal degradation of whey ultrafiltration permeate, or pure lactose, was investigated in the solid-state and in solution (Table 1). The concentration was 9.9% w/w for all the solutions. This investigation was performed to study the impact of pH on the secondary reactions that occur during the reaction of the lactose in the whey ultrafiltration permeate with acids (Buera *et al.* 1987; Sun *et al.* 2019; Zhao *et al.* 2019). In the presence of nitrogenous substances, such as urea in permeate powder, the carbonyl group of lactose can be involved in the Maillard reaction ((Ames 1998; Echavarría et al. 2012; Murata 2021; Yaylayan 1997). Sugars also undergo caramelization when heated. Acid medium also favors sugar caramelization. Therefore, this study aimed to examine the secondary reactions that could occur during the esterification of the lactose contained in whey ultrafiltration permeate and lactose with carboxylic acids.

The powders and solutions were heated at 160 °C for 3 h, and after cooling down, they were analyzed by FTIR following the analysis parameters as for the products obtained after esterification of whey ultrafiltration permeate or lactose with biosourced acids.

Table 1. Samples Used to Study the Thermal Degradation of Whey ultrafiltration permeate and Lactose

Sample description	рН
Whey UF permeate powder	
Whey UF permeate solution	5.6
Whey UF permeate acid solution	2.3
Whey UF permeate alkaline solution	11.3
Lactose powder	
Lactose solution	5.2
Lactose acid solution	2.5
Lactose alkaline solution	10.9

Solid-state Synthesis of Lactose-based Polyesters with Various Acids

The reaction was carried out first separate from the wood using acids with different melting points, as presented in Table 2. The carboxylic acids selected (CA, FA, MA, and SA) were either mixed with whey ultrafiltration permeate powder or pure lactose powder in an aluminum pan at an OH:COOH molar ratio of 1:1. The mixtures were then submitted to the curing process in a preheated oven at 140 or 160 °C for a duration of 3 h. Two curing temperatures were selected to investigate the factors influencing this reaction and gain a better understanding of the reactivity of lactose in whey ultrafiltration permeate with acids before treating the wood. The resulting samples were labelled as given in Table 3. After the curing process, the samples were removed from the oven, allowed to cool down, and stored in a desiccator before undergoing characterization analysis.

Trembling Aspen Sawdust Treatment

This study focused on the three following aspects: 1) the impact of the curing temperature (treatment with water alone *vs.* other treatments), 2) the influence of minor components other than lactose in the whey ultrafiltration permeate (treatment with permeate *vs.* pure lactose alone), and 3) the synergistic effects of malic acid and whey ultrafiltration permeate (treatment with permeate and malic acid *vs.* malic acid alone) on the properties of the sawdust post-treatment.

Table 2. Physical and Chemical Properties of Lactose and the Biobased Acids

Molecule	Solubility in water at 20 °C (g/L)	рКа	Melting point (°C)	Degradation temperature (°C)	Structure
Lactose	187		201-202		CH ₂ OH OH OH OH
Citric acid (CA)	592	3.13, 4.76 and 6.40	153	175	но он он
Fumaric acid (FA)	4.9	3.03 and 4.44	287	200 (sublime)	НОООН
Malic acid (MA)	558	3.46 and 5.10	131-132	140	НО ОН
Succinic acid (SA)	70	4.16 and 5.61	184	235	НОООН

Table 3. Experimental Conditions (Mixture, Temperature) for the *ex situ* Esterification of the Lactose in the Whey ultrafiltration Permeate and Pure Lactose with Citric, Fumaric, Malic, and Succinic Acids

Mixture		Curing temperature	Assignment
Carboxylic acid	Lactose source	(°C)	
Citric acid (CA)	Whey UF permeate	140	CAP140
	powder	160	CAP160
	Lactose powder	140	CAL140
	•	160	CAL160
Fumaric acid (FA)	Whey UF permeate	140	FAP140
	powder	160	FAP160
	Lactose powder	140	FAL140
		160	FAL160
Malic acid (MA)	Whey UF permeate	140	MAP140
	powder	160	MAP160
	Lactose powder	140	MAL140
		160	MAL160
Succinic acid (SA)	Whey UF permeate	140	SAP140
	powder	160	SAP160
	Lactose powder	140	SAL140
		160	SAL160

First, 5 g of trembling aspen (*Populus tremuloides* Michx.) sawdust were immersed in five different solutions: water, malic acid, whey ultrafiltration permeate, whey ultrafiltration permeate, and malic acid (referred to as AMPUL), and lactose aqueous solutions. The sawdust was used because it is easy to handle, allowing better control of reaction parameters (time, temperature, concentration, and homogeneity). The malic acid solution had a concentration of 35.5% w/w, the permeate and lactose solutions were at 16.7% w/w due to the limited solubility of lactose in water, and the AMPUL solution contained 16.7% w/w of permeate powder and 25.9% w/w of malic acid.

A fine mesh screen was used to keep the sawdust immersed in the solutions. The samples were then placed under a dynamic vacuum of 50 mbar for 1 h. After the vacuum was released, the samples were left for 24 h in the solutions to absorb at room temperature and atmospheric pressure. The sawdust was subsequently removed from the solution and dried for 48 hours in a conditioned chamber (21 °C, 41% RH). Following the drying process, the sawdust samples were heated at 160 °C for 24 h. A summary of the sawdust treatment process is provided in Fig. 2.

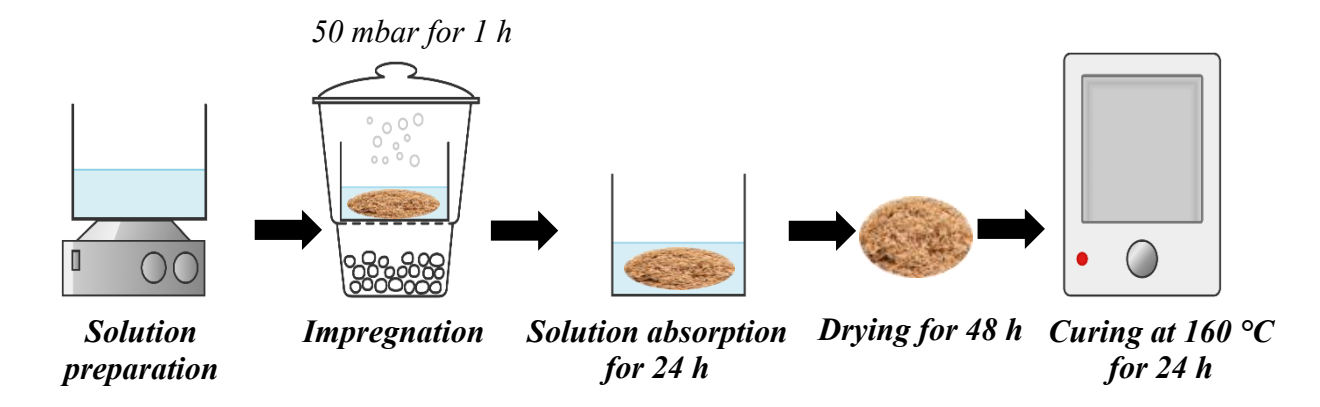


Fig. 2. Process of sawdust treatment with different solutions

Characterization

Fourier transform infrared spectroscopy (FTIR)

Fourier transform infrared spectroscopy analysis was conducted using the Invenio R spectrometer (Bruker, Billerica, MA, USA). It was first performed to investigate whether the lactose in the whey UF permeate caramelizes at 160 °C, or if the Maillard reaction occurs under these specific conditions. FTIR also allowed the determination of whether esterification occurred between lactose and the selected carboxylic acids. Finally, FTIR was employed to analyze the sawdust after treatment with each solution, allowing the identification of chemical transformations. Spectra were obtained by accumulating 32 scans in the 400 to 4000 cm⁻¹ region, with a resolution of 4 cm⁻¹. The OPUS software (Bruker, Billerica, MA, USA) was used to process the spectra.

¹³C Cross-polarization magic angle spinning nuclear magnetic resonance spectroscopy (¹³C CP/MAS NMR)

As the esterification products formed were found to be insoluble in most solvents, they were analyzed using solid-state ¹³C-NMR to confirm the FTIR results. Spectra were recorded using a Bruker Avance 400 MHz spectrometer (Bruker Biospin, Milton, ON, Canada) with a 4 mm magic angle spinning (MAS) probe at a rotational speed of 10 kHz.

The carbon cross polarisation MAS (CPMAS) experiment was performed with a contact time of 1 ms, and a two-pulse phase modulation (TPPM) decoupling scheme of 96 kHz was used. An external adamantane reference was applied to the recorded spectra. Only samples cured at 160 °C with whey ultrafiltration permeate were analyzed, as samples cured at 140 °C led to similar results to those cured at 160 °C. Additionally, uncured mixtures of whey ultrafiltration permeate with the four carboxylic acids, noted as CAP (for CA and whey ultrafiltration permeate), FAP (for FA and whey ultrafiltration permeate), MAP (for MA and whey ultrafiltration permeate), and SAP (for SA and whey ultrafiltration permeate), were analyzed for comparison.

Thermogravimetric analysis (TGA) and derivative thermogravimetry (DTG)

Thermogravimetric analyses were performed using a TGA 851e (Mettler Toledo, Greifensee, Switzerland) to assess the thermal degradation of the starting materials (e.g., acids, whey ultrafiltration permeate, and pure lactose) and the polyesters prepared. Additionally, the analyses aimed to evaluate the changes in the thermal degradation of treated sawdust and the impact of curing temperature on the thermal properties of wood sawdust. The temperature was raised from 35 to 600 °C at a rate of 10 °C/min under a nitrogen flow of 100 mL/min for lactose powder, whey ultrafiltration permeate powder, and the products obtained after their thermal degradation as well as for the acids, and the products obtained after their reaction at 160 °C. Each sample was tested two times. For untreated and treated sawdust, the temperature was raised from 35 to 800 °C at a rate of 10 °C/min under a nitrogen flow of 100 mL/min.

Vapor Sorption Isotherm Experiments

Sorption and desorption isotherm tests were conducted using a DVS Adventure water vapor sorption analyzer (Surface Measurement Systems, Allentown, USA) at 25 °C. The samples were initially conditioned at 0% relative humidity (RH) to allow for mass stabilization. Subsequently, the RH was increased from 0% to 95% in 10% increments and then decreased using the same increments. The RH in the analysis chamber was maintained until the sample's mass percentage varied by less than 0.0002% over 5 minutes or the step duration exceeded 24 h. The moisture content during adsorption and desorption cycles was plotted against the target RH. Two repetitions were performed for untreated sawdust and sawdust treated with each solution. The results for treated sawdust were compared to those for untreated sawdust to assess the impact of each treatment on the wood's hygroscopic behavior.

RESULTS AND DISCUSSION

Thermal Degradation of Permeate Powder and Lactose

Colored residues were obtained following thermal degradation experiments of various whey ultrafiltration permeate and lactose solutions, as illustrated in Fig. 3. This corroborates the assumption that caramelization of the lactose occurs during heating, along with the Maillard reaction involving the lactose and nitrogenous substances present in the whey ultrafiltration permeate. In Fig. 3, heated whey ultrafiltration permeate transitions to a brown hue (Fig. 3a and 3b), whereas lactose alone maintained a predominantly white appearance after heating at 160 °C (Fig. 3e and 3f). This discrepancy indicates that the Maillard reaction could occur in the whey ultrafiltration permeate upon heating.

Furthermore, under acidic conditions (Fig. 3c and 3g), both whey ultrafiltration permeate and lactose turned very dark, suggesting that lactose undergoes caramelization under acidic conditions when heated to 160 °C (Kroh 1994; Swift 2023).

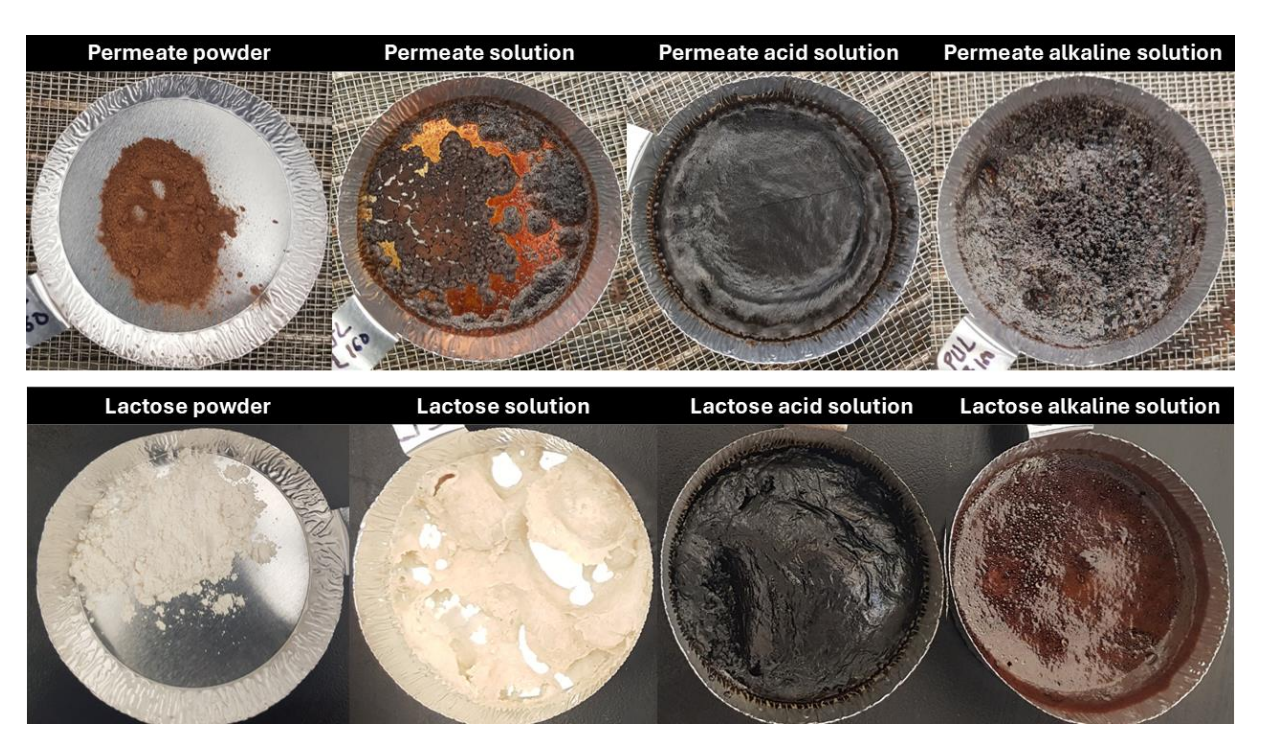


Fig. 3. Powder and solutions of whey ultrafiltration permeate and lactose heated at 160 °C

Fourier transform infrared spectroscopy analysis of permeate powder, lactose, and the products of their thermal degradation

Compounds resulting from the thermal degradation of whey ultrafiltration permeate, as well as pure lactose in different media were analyzed by FTIR, and the spectra of the region of interest are presented in Fig. 4. The full spectra can be seen in the supplementary information. When whey ultrafiltration permeate was heated, a new band emerged at around 1710 cm⁻¹, indicating a potential Maillard reaction (Amadori products) between nitrogenous substances and lactose in the whey ultrafiltration permeate (Nielsen *et al.* 2022). However, the only difference observed between lactose heated to 160 °C and untreated lactose was the band's disappearance at 1656 cm⁻¹, corresponding to water absorbed in the lactose structure, indicating lactose dehydration, meaning no reaction occurs. The lactose acid solution and whey ultrafiltration permeate acid solution exhibited similar spectra after curing at 160 °C. For these two samples, a significant decrease in the band's intensity at 1033 cm⁻¹ corresponding to the main band of carbohydrates was observed, along with a significant decrease in the intensity of the broad band around 3300 cm⁻¹ corresponding to the OH groups.

Additionally, new bands appeared at 1577, 1664, and 1702 cm⁻¹. These bands are attributed to the aromatic group, C=C double bonds, and C=O group, respectively. It is known that sugar caramelization leads to the creation of furan-based moieties (Sun *et al.* 2019; Zhang *et al.* 2012) and further to a complex aromatic molecule named *humin*, which is a complex aromatic branched polymer (Shen *et al.* 2020; Xu *et al.* 2020; Ye *et al.* 2024). The FTIR spectra obtained support the hypothesis that lactose caramelized under these pH and temperature conditions (Sengar and Sharma 2014).

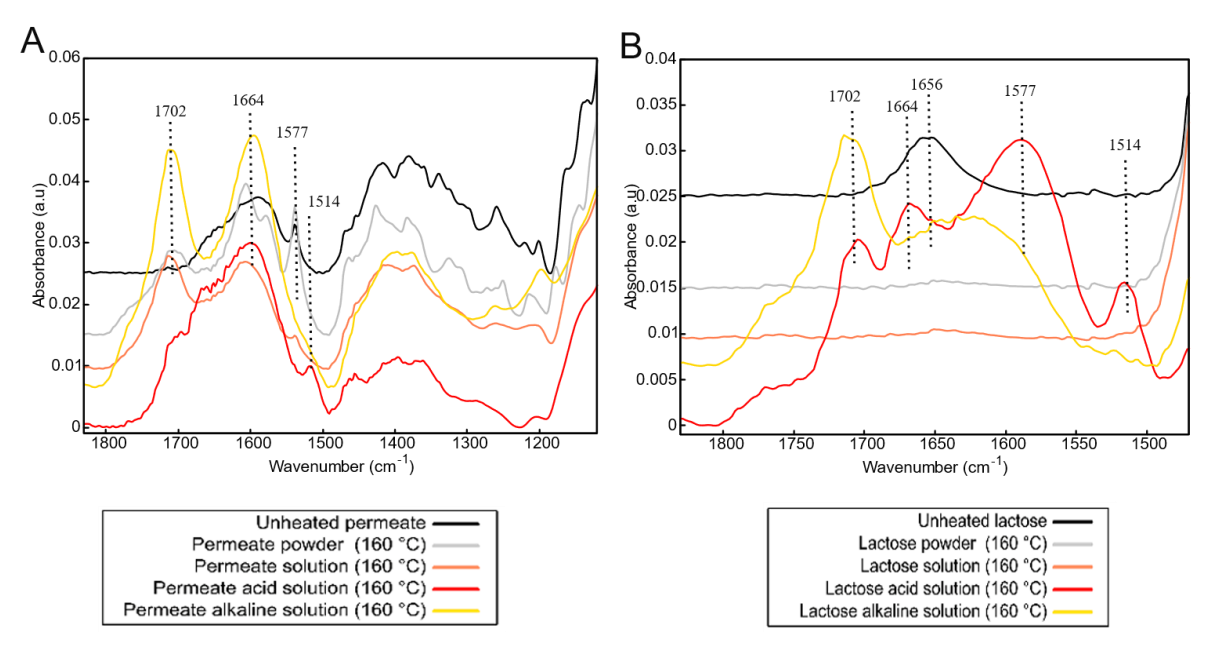


Fig. 4. FTIR spectra of the region of interest of products from the thermal degradation of whey ultrafiltration permeate (a) and lactose (b)

Thermogravimetric analysis and derivative thermogravimetry of permeate powder, lactose, and the products of their thermal degradation

Figure 5 illustrates the TGA results for the products obtained from the thermal degradation of whey ultrafiltration permeate and pure lactose in various media, with corresponding data compiled in Table 4. Whey ultrafiltration permeate and pure lactose exhibited distinct thermal behaviors, with whey ultrafiltration permeate demonstrating a lower initial pyrolysis temperature than lactose. Additionally, whey ultrafiltration permeate displayed a greater residual mass after degradation at 600 °C compared to lactose, attributed to the minerals present, particularly calcium phosphate. Phosphorus, which is commonly employed as a flame retardant, accelerates dehydration, thereby lowering the initial pyrolysis temperature and facilitating the formation of substantial char (residual mass). In contrast, both whey ultrafiltration permeate acid solution, and lactose acid solution exhibited similar thermal behaviors after curing. This reaffirms the caramelization undergone by lactose in whey ultrafiltration permeate and pure lactose. Their initial pyrolysis temperature mirrors that of whey ultrafiltration permeate and lactose, with almost 50% stable residual mass observed after degradation at 600 °C. Furthermore, the degradation curve slope in ATG for whey ultrafiltration permeate acid solution, and lactose acid solution after curing was lower compared to whey ultrafiltration permeate and lactose, indicating that compounds formed after heating to 160 °C were more thermally stable. Caramelization and the Maillard reaction typically yield compounds with aromatic rings (Shen et al. 2020; Sun et al. 2019; Xu et al. 2020), providing insight into the enhanced thermal stability observed in compounds obtained from heating acid whey ultrafiltration permeate and acid lactose at 160 °C.

Table 4. TGA Data for Whey ultrafiltration Permeate, and Lactose and the Products of their Thermal Degradation in Different Conditions

Sample	Initial Degradation Temperature (°C)	Maximum Degradation Rate Temperature (°C)	Residual Mass after 800 °C (%)
Whey UF permeate	194 ± 5	128, 220	32 ± 1
Whey UF permeate powder heated at 160 °C	198 ± 5	75, 227	37 ± 0
Whey UF permeate acid solution heated at 160 °C	50 ± 1 and 180 ± 1	84, 273	49 ± 0
Whey UF permeate alkaline solution heated at 160 °C	181 ± 1	95, 210, 337	43 ± 0
Lactose	220 ± 7	128, 251, 310	20 ± 4
Lactose heated at 160 °C	227 ± 1	248, 312	22 ± 1
Lactose acid solution heated at 160 °C	59 ± 6 and 185 ± 2	88, 303	48 ± 1
Lactose alkaline solution heated at 160 °C	194 ± 1	111, 215, 348	28 ± 0

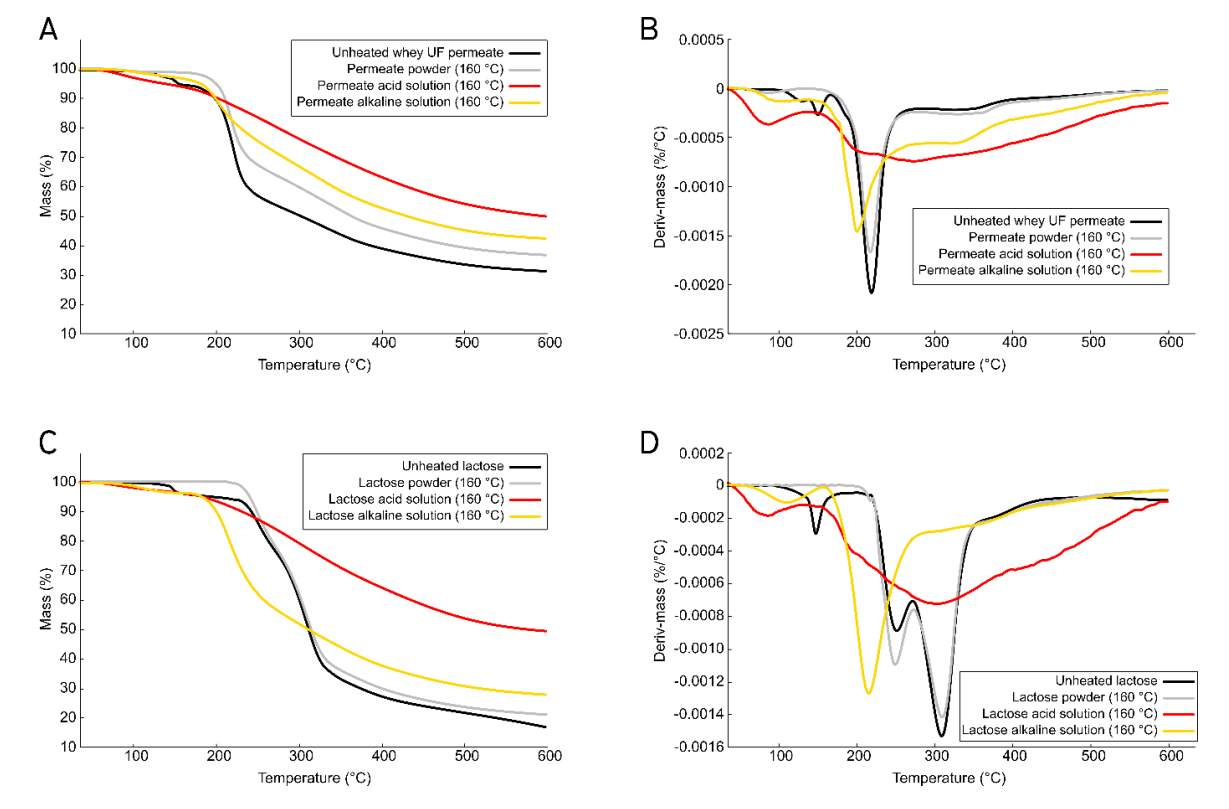


Fig. 5. Thermogravimetric analysis (A-C) and its derivative (B-D) for products obtained after curing of different whey ultrafiltration permeate samples (A-B) and different lactose samples (C-D) at 160 °C

Solid-state Synthesis of Lactose-based Polyesters with Various Acids

After the curing, for the whey ultrafiltration permeate mixtures, regardless of the temperature (140 °C or 160 °C), brittle solids ranging from pale for the citric acid-

containing mixtures to very dark for the succinic acid-containing mixtures were obtained, as depicted in Fig. 6. However, some of the mixtures with pure lactose did not change color after the curing. This was observed for all mixtures containing fumaric acid cured at 140 and 160 °C and the mixture with succinic acid heated at 140 °C. Taking into consideration the melting points of the different reactants used, it was concluded that the melting of one of the reactants is necessary to initiate the esterification reaction. In contrast, the mixture of whey ultrafiltration permeate with succinic acid heated at 140 °C turned dark due to ash and non-protein nitrogen contained in whey ultrafiltration permeate, which are considered impurities that can melt at 140 °C, facilitating the reaction of these two compounds. This capability is absent for pure lactose. Mixtures containing fumaric acid did not react at all for both the lactose and the whey ultrafiltration permeate, as the melting points of fumaric acid and lactose are 287 and 202 °C, respectively, meaning heating them at 140 °C or 160 °C would not enable this reaction.

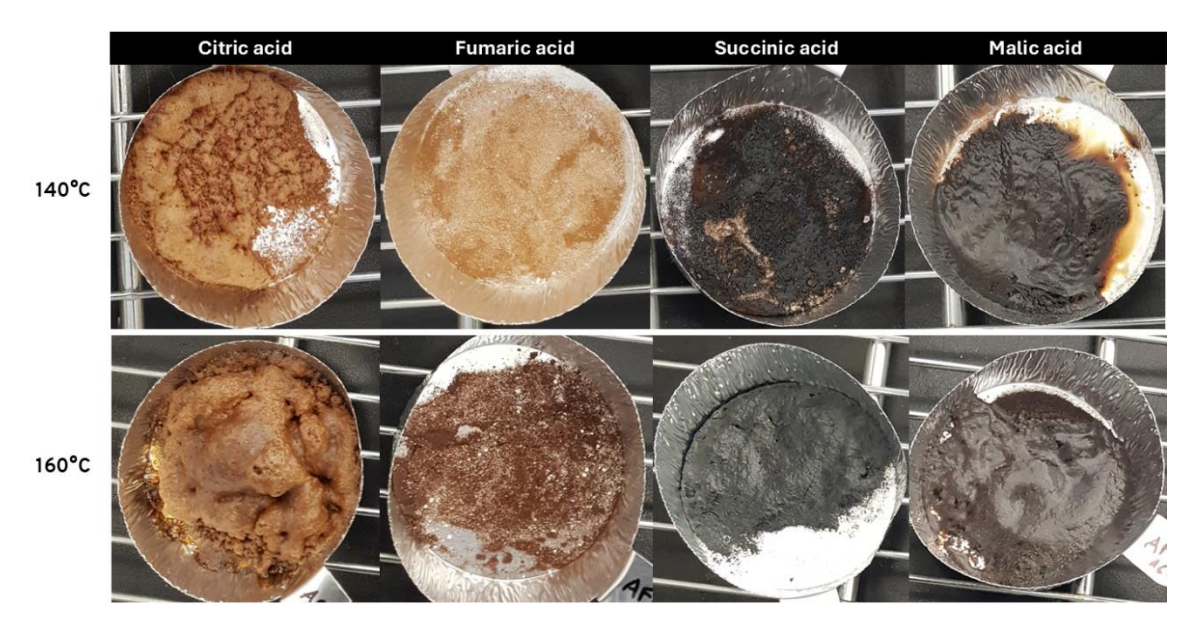


Fig. 6. Pictures of the products of the reaction of whey ultrafiltration permeate with different acids

The color change was found to be closely related to the acid used, thus the acidity, and is attributed to secondary reactions that may occur during the heating. Sugars tend to caramelize when heated to high temperatures in an acidic environment (reference lactose caramelization). Moreover, reducing sugars, such as lactose, tend to undergo the Maillard reaction in the presence of nitrogen compounds, generally forming brown-colored compounds. Consequently, products obtained from whey ultrafiltration permeate exhibited colors ranging from pale to very dark, depending on the acid used, compared to those obtained from pure lactose, which are uniformly dark (Fig. 7). Two origins of coloring are identified: caramelization and the Maillard reaction in the case of whey ultrafiltration permeate, and solely caramelization in the case of lactose. The pure lactose used in this study contains no nitrogenous substances, as shown in Table 5. Therefore, the observed coloration can be attributed solely to caramelization.

Table 5. Analysis of the Carbon, Nitrogen, and Sulphur Content of Whey ultrafiltration Permeate and Lactose

	%C	%N	%S
Lactose	41.9 ± 0.1	0.00	0.01 ± 0.01
Whey UF permeate	38.7 ± 0.2	0.2 ± 0.0	0.07 ± 0.00

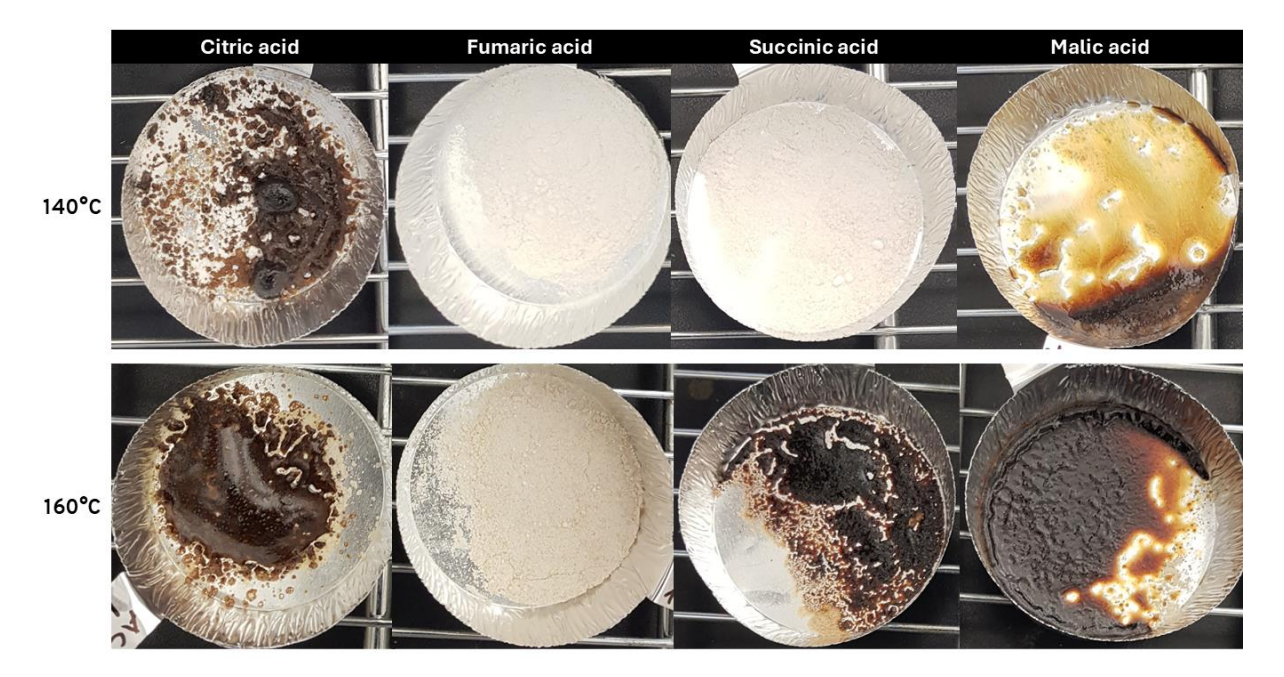


Fig. 7. Pictures of the products of the reaction of lactose with different acids

Fourier Transform Infrared Spectroscopy Analysis of the Various Acids and the Products of their Reaction with Lactose and Permeate Powder

Figure 8 presents the FTIR spectra of compounds obtained after the reaction of whey ultrafiltration permeate with different acids and those obtained after the reaction of pure lactose with the same acids. For each spectrum, the C=O region in the range 1654 to 1740 cm⁻¹ and the ether bond around 1160 cm⁻¹ were analyzed. Two main trends were observed: on the one hand, there were mixtures that reacted during curing, and on the other hand, those that did not react during curing. For all products obtained after the reaction of pure lactose or lactose from whey ultrafiltration permeate with citric acid (Fig. 8a) and malic acid (Fig. 8c), a band between 1161 and 1173 cm⁻¹ appeared for citric acid-based compounds and malic acid-based compounds due to ether bond formation. Additionally, the C=O acid peaks at 1685 cm⁻¹ for citric acid and 1673 cm⁻¹ for malic acid shifted towards the C=O ester peaks at 1720 cm⁻¹ and 1717 cm⁻¹, respectively, after the reaction. Similar observations were made for all mixtures with succinic acid (Fig. 8d), except for the mixture containing pure lactose and succinic acid heated to 140 °C (ASL140). In Fig. 8b, the spectra of mixtures containing fumaric acid showed none of these observations. This indicates that pure lactose or lactose contained in whey ultrafiltration permeate reacts with malic acid and citric acid when heated to 140 or 160 °C. Succinic acid can also react with pure lactose and lactose in whey ultrafiltration permeate, except for the mixture of succinic acid and pure lactose heated to 140 °C. In the case of fumaric acid, the reaction does not occur regardless of whether it is heated to 140 or 160 °C. This is attributed to the requirement that one of the products must melt to initiate the reaction. For all the products obtained after the reaction with citric acid, malic acid, and succinic acid (except for the combination of succinic acid and pure lactose at 140 °C), a decrease in the band's intensity at 1033 cm⁻¹ was observed. This band is characteristic of the C-O-C carbohydrate signal, indicating that the lactose underwent degradation through caramelization.

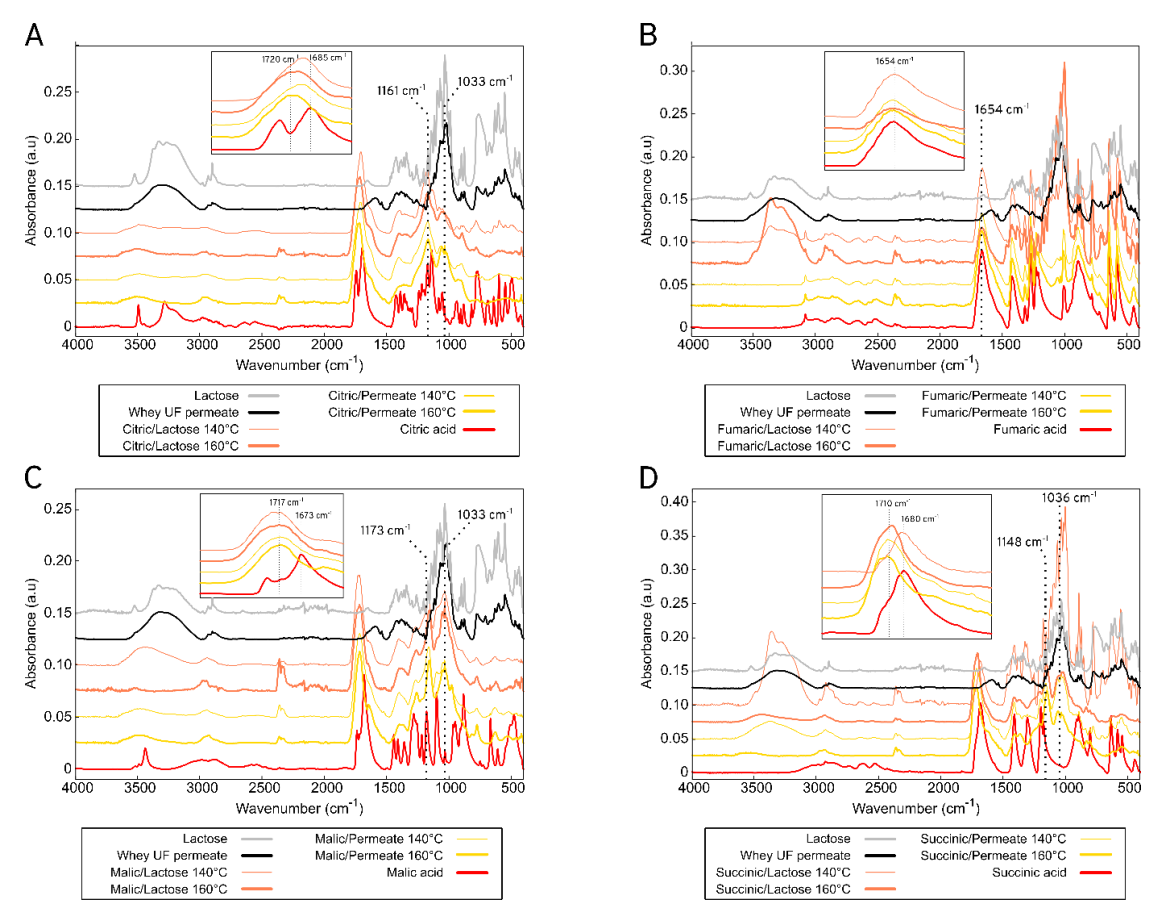


Fig. 8. FTIR spectra of the products of the reaction of CA with whey ultrafiltration permeate and lactose (a), FA with whey ultrafiltration permeate and lactose (b), MA with whey ultrafiltration permeate and lactose (c) and AS with whey ultrafiltration permeate and lactose (d)

¹³C CP/MAS Solid-state NMR of the Various Acids and the Products of their Reaction with Permeate Powder

CAP160, FAP160, MAP160, and SAP160 were analyzed by ¹³C CP/MAS solid-state NMR and compared to their respective mixtures without heating, namely CAP, FAP, MAP, and SAP. The spectra are presented in Fig. 10. Monitoring the acidic C=O band (around 180 ppm) and the C₆ (and C₆) band (62 ppm) of the carbohydrates (Earl and Parrish 1983) (see Fig. 9) allows for evaluation of the reaction progress. In Fig. 10a, CAP160 exhibits a different spectrum from the CAP mixture (CA + whey ultrafiltration permeate mixture without heating). The acid C=O band (180 ppm) in CA has been converted to an ester C=O band (174 ppm) in CAP160. Additionally, the disappearance of the C₆ band in CAP160 indicates displacement of this band due to the reaction of lactose in whey ultrafiltration permeate with CA. Similar observations were made for MAP160 (Fig. 10c) and SAP160 (Fig. 10d). For the mixture containing MA, a shift of the acid C=O band from 181 ppm to the ester C=O band at 174 ppm was observed. The carbohydrate C₆ band also overlaps with the C₂, C₃, and C₅ carbohydrate bands at 72.6 ppm.

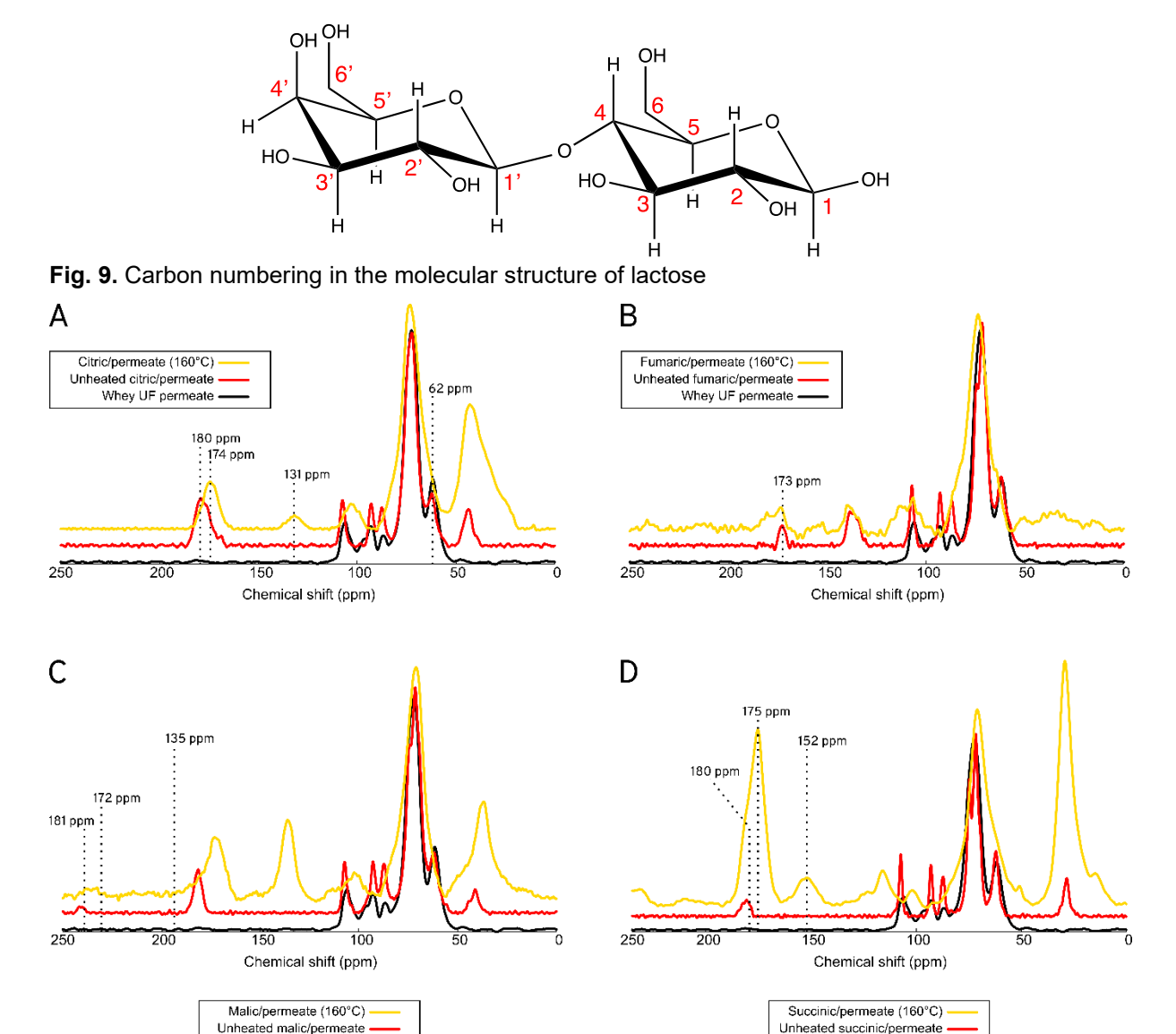


Fig. 10. Solid-state NMR spectra of mixtures of CA and whey ultrafiltration permeate cured and uncured (a), FA and whey ultrafiltration permeate cured and uncured (b), MA and whey ultrafiltration permeate cured and uncured (c) and SA and whey ultrafiltration permeate cured and uncured (d)

In Fig. 10d, the acid C=O band of SA, previously located at 180 ppm, shifts to 175 ppm, indicating an esterification reaction between lactose in whey ultrafiltration permeate and SA. However, no difference in the acidic C=O band was observed before and after heating for FAP160 (Fig. 10b), confirming the FTIR results that CA, MA, and SA reacted with lactose in whey ultrafiltration permeate to form esters at 160 °C. The likely reason for this is the requirement for melting of one of the compounds to complete this reaction, consistent with previous FTIR results. The NMR analysis also supports the presence of secondary reactions during the esterification of lactose in whey ultrafiltration permeate with acids. In the NMR spectra of CAP160, MAP160, and SAP160, a new band appears between 130 and 152 ppm, which can be attributed to C=C, CN, CNH2, and cyclic compounds in the NMR table.

Thermogravimetric analysis and derivative thermogravimetry of the various acids and their reaction products with lactose and permeate powder

The TGA and DTG curves are illustrated in Fig. 11. The initial temperature of degradation, temperature at the maximum degradation rate, and residual weight after degradation, are given in Table 6. Significantly divergent thermograms were observed between the starting materials and the resultant products. Whey ultrafiltration permeate initiated degradation earlier than pure lactose. This can be potentially attributed to the presence of phosphate moieties in whey ultrafiltration permeate, which may lower the initial pyrolysis temperature of lactose. The residual mass after 600 °C underscores the impact of phosphate on the thermal behavior of whey ultrafiltration permeate. Phosphate moieties are commonly employed as fire-retardant agents, promoting earlier degradation and facilitating the formation of char (Hagen *et al.* 2009). This phenomenon may elucidate why lactose in whey ultrafiltration permeate, together with SA, can react at 140 °C, whereas pure lactose and SA fail to do so, as whey ultrafiltration permeate may degrade at lower temperatures due to its mineral content.

Table 6. TGA Data of Acids, Whey ultrafiltration Permeate, Lactose, and the Products of their Respective Reaction

Samples	Initial Degradation Temperature (°C)	Maximum Degradation Rate Temperature (°C)	Residual Mass after 600 °C (%)
CA	185 ± 6	225	4.2 ± 1
FA	235 ± 1	307	0
MA	188 ± 1	250 and 282	0
SA	197 ± 1	265	0
Whey UF permeate	194 ± 5	220	32 ±1
Lactose	220 ± 7	251 and 310	20 ± 4
CAP160	194 ± 1	232 and 350	35.1 ± 2
CAL160	210 ± 6	255 and 350	23.8
FAP160	200 ± 4	260	21.9 ± 1
FAL160	200 ± 6	251	16.9 ± 2
MAP160	187 ± 8	226 and 310	31.7 ± 2
MAL160	230 ± 8	274	23.7 ± 1
SAP160	175 ± 7	225 and 337	35.1 ± 2
SAL160	228 ± 7	296	20.5 ± 1

CA exhibited initial degradation at 185 °C, with the maximum degradation rate observed at 225 °C, as evidenced by the DTG curve. CAP160 displayed a lower initial degradation temperature than CAL160. This was potentially due to the presence of minerals, including phosphate, in whey ultrafiltration permeate. The residual weight after 600 °C of CAP160 was higher than that of CAL160, suggesting greater thermal stability compared to the initial reactants. FA began degradation at 235 °C, with a maximum degradation rate observed at 307 °C. FAP160 and FAL160 exhibited similar thermograms, with degradation initiating at 200 °C and a maximum degradation rate observed at 260 and 251 °C, respectively.

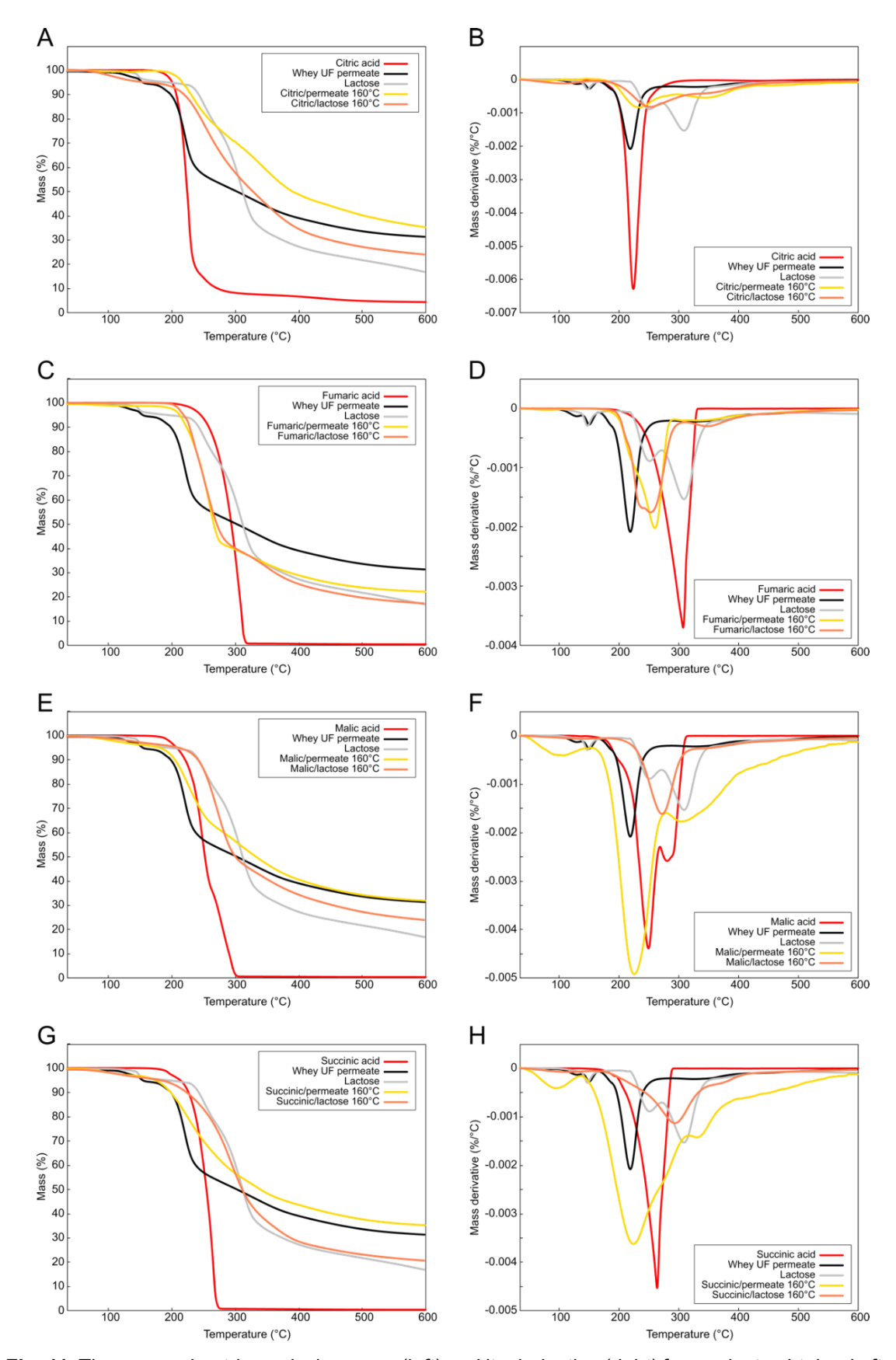


Fig. 11. Thermogravimetric analysis curves (left) and its derivative (right) for products obtained after curing with citric acid (A-B), fumaric acid (C-D), malic acid (E-F), and succinic acid (G-H)

Both retained a substantial percentage of their weight after degradation at 600 °C. While FTIR and NMR results indicated that FA did not react with lactose at 160 °C, thermograms suggest that heating above 200 °C, which is above the melting point FA (187 °C), allowed the two compounds to react before undergoing degradation. The products of the reaction of MA and SA with lactose and whey ultrafiltration permeate exhibited similar thermal behavior. MAP160 and SAP160 commenced degradation earlier than MAL160 and SAL160, respectively. This was likely due to the mineral content of whey ultrafiltration permeate, notably calcium phosphate. ATG corroborates NMR and FTIR results. If lactose fails to react with these acids, the thermograms should exhibit distinct peaks for lactose and the acid due to their differing thermal behaviors. However, this was not the case. In formulations containing FA, TGA serves as a tool enabling reaction with lactose before degradation occurs during heating.

Based on the aforementioned findings, three scenarios have been identified for the esterification of lactose in whey ultrafiltration permeate with acids:

- 1. Polycondensation at reactant melting point: At the melting point of one of the reactants, lactose in whey ultrafiltration permeate, and acids having two carboxylic groups or more undergo polycondensation to form polyesters.
- 2. Maillard reaction with whey ultrafiltration permeate components: Upon heating of whey ultrafiltration permeate alone, lactose and nitrogenous substances within the whey ultrafiltration permeate react *via* the Maillard reaction, forming complex browning compounds.
- 3. Caramelization in acidic medium: The final scenario involves the caramelization of lactose in whey ultrafiltration permeate within an acidic environment at high temperatures, leading to the production of darker and thermally stable compounds.

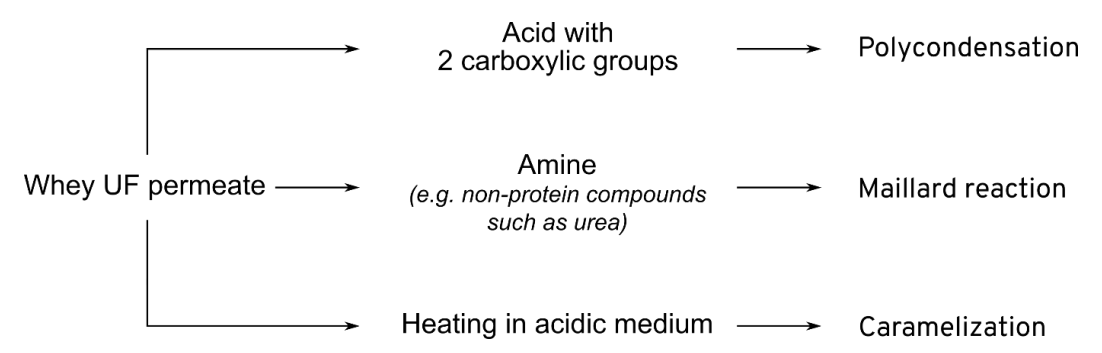


Fig. 12. Summary of the scenarios occurring during the esterification of the lactose in the whey ultrafiltration permeate

Trembling Aspen Sawdust Treatment

In the preceding section, the reaction of lactose in whey ultrafiltration permeate with acids such as MA, CA, and SA, resulted in the formation of polyesters when cured at 160 °C. This section explores the impact of this reaction on the hygroscopic and thermal properties of wood sawdust using MA and whey ultrafiltration permeate on trembling aspen (*Populus tremuloides*) sawdust. Figure 13 showcases photographs of untreated trembling aspen sawdust and sawdust treated with each respective treatment. Following treatment, all samples exhibited a color change compared to untreated sawdust. Sawdust treated with water assumed a light-yellow hue, resembling pristine wood (Fig. 13b). This color change during water treatment primarily results from the migration or diffusion of extractives to the surface (Sundqvist and Morén 2002; Shi *et al.* 2018). Treatment with

malic acid imparts a dark chocolate-brown color to the sawdust, attributed to acid treatment hydrolyzing certain wood polymers (Shi *et al.* 2018) and inducing a black-like appearance (Fig. 13c). Additionally, the sawdust became thinner due to acid hydrolysis. Whey ultrafiltration permeate treatment resulted in a brown coloration of the sawdust (Fig. 13d), which can be attributed to the reaction between whey ultrafiltration permeate components, notably the Maillard reaction between lactose and non-protein nitrogen substances. This coloration mirrors observations when whey ultrafiltration permeate powder alone is heated at 160 °C. Treatment with lactose yielded a light brown coloration, likely due to a combination of extractive migration, water, and heat effects on lactose (Fig. 13e). Conversely, sawdust treated with AMPUL exhibited a dark coloration (Fig. 13f), potentially stemming from a combination of lactose caramelization and Maillard reaction product coloration. Notably, sawdust treated with AMPUL retains its shape compared to malic acid-treated sawdust, which becomes thinner post-treatment.

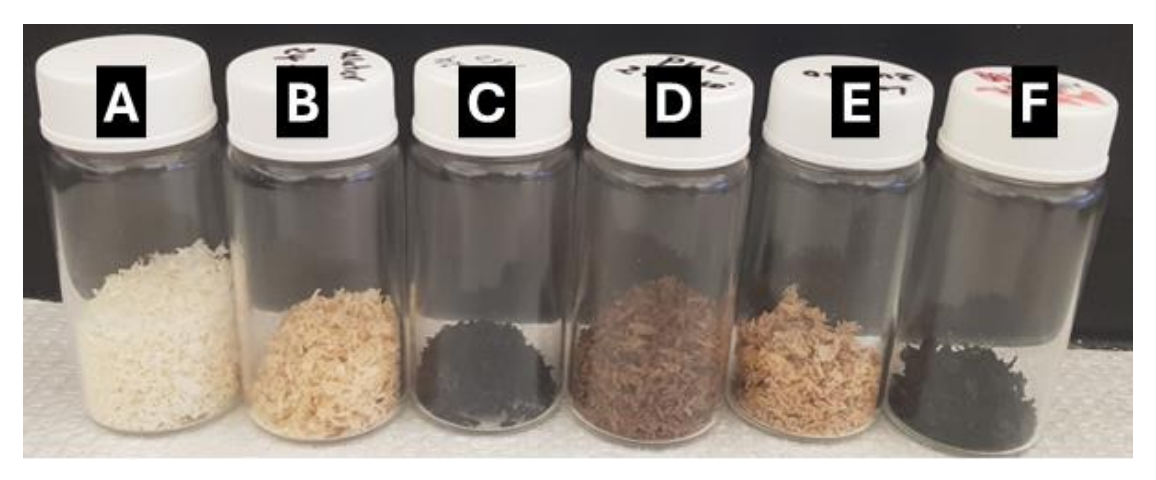


Fig. 13. Photographs of untreated sawdust (a) and sawdust treated: with water (b), with malic acid (c), with whey ultrafiltration permeate (d), with lactose (e) and with AMPUL (f)

Fourier transform infrared spectroscopy analysis of untreated trembling aspen sawdust and trembling aspen sawdust treated with different solutions

Figure 14 presents the FTIR spectra of untreated trembling aspen sawdust and sawdust treated with various solutions. The spectra of the untreated sawdust and sawdust treated with water exhibited similarities, indicating that the treatment temperature (160 °C) did not significantly alter the main wood components (cellulose, hemicelluloses, lignin) (Elrhayam and El Bachiri 2024). Similarly, the spectrum of sawdust treated with lactose closely resembled that of the untreated sample, with a notable increase in the band's intensity at 1030 cm⁻¹ corresponding to C-O-C in carbohydrates. This increase is attributed to the addition of lactose, which contains this functional group and remains unchanged in trembling aspen sawdust during curing at 160 °C. For sawdust treated with whey ultrafiltration permeate, new intense bands emerged at 1530, 1562, and 1607 cm⁻¹, indicative of C=C double bonds of the aromatic ring. This suggests that compounds from the whey ultrafiltration permeate reacted within the wood, generating new products. The spectra of sawdust treated with AMPUL and malic acid exhibited similarities, characterized by a significant increase in band intensity at 1733 cm⁻¹ corresponding to the C=O ester, along with a notable decrease in intensity of the broad band around 3300 cm⁻¹. This indicates the reaction of malic acid with free OH groups in the wood cell wall. Additionally, the AMPUL-treated sample displays an increased intensity at 1419 cm⁻¹, suggesting a reaction between whey ultrafiltration permeate components and wood cell wall OH groups, a phenomenon not observed in malic acid treatment alone. This observation aligns with treatment involving whey ultrafiltration permeate alone. These findings demonstrated that the same reactions observed outside the wood for each of its components also occurred within the wood matrix. Consequently, it is crucial to investigate the impact of these reactions on wood properties, such as hygroscopicity and thermal behavior.

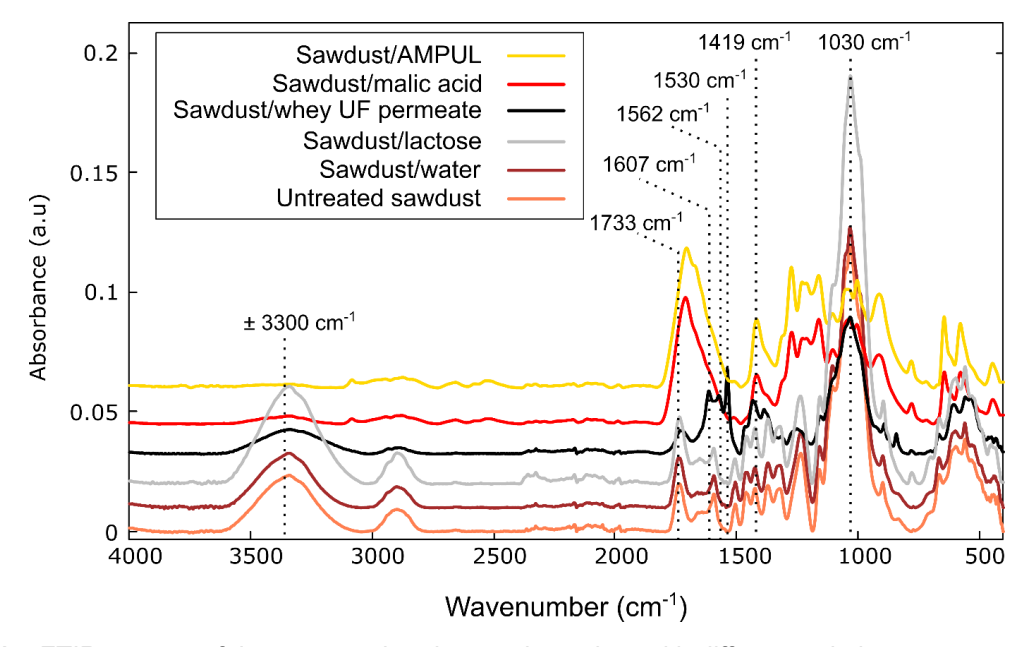


Fig. 14. FTIR spectra of the untreated and treated sawdust with different solutions

Thermogravimetric analysis and derivative thermogravimetry of untreated trembling aspen sawdust and trembling aspen sawdust treated with different solutions

Thermogravimetric analysis was performed to examine the thermal behavior of sawdust treated with various solutions and compare it to untreated sawdust (Fig. 15). Given wood's sensitivity to heat and acid treatment, this analysis enables the assessment of the treatment's impact on wood's thermal characteristics. The results are summarized in Table 7. Treatment with water did not alter the sawdust's thermal behavior significantly. The initial pyrolysis temperature, temperatures at maximum degradation rates, and residual mass after 800 °C remained consistent with untreated wood. However, a weight loss at 66 °C was observed in untreated sawdust, which can be attributed to the dehydration of absorbed water. This discrepancy arises as water-treated sawdust was stored in a desiccator with silica gel, while untreated sawdust was stored in a conditioning room (41% RH, 21 °C). In contrast, treatments with malic acid, whey ultrafiltration permeate, and AMPUL reduce the initial pyrolysis temperature. This decrease results in a higher residual mass formation compared to untreated and water-treated samples. Specifically, the residual masses were 21, 22, and 30% for AMPUL, malic acid, and whey ultrafiltration permeatetreated samples, respectively. These findings underscore the influence of different treatments on the thermal properties of sawdust, highlighting the potential of whey ultrafiltration permeate treatments to modify wood's thermal behavior.

Table 7. TGA Data for Untreated Sawdust and Sawdust Treated with Different Solutions

Sample	Initial Degradation Temperature	Maximum Degradation rate Temperature	Residual Mass after 800 °C (%)
Untreated sawdust	268 ± 1	66, 339 and 472	8.3 ± 9
Sawdust treated with water	268 ± 1	339 and 472	8.0 ± 8
Sawdust treated with malic acid	210 ± 0	250 and 328	22.0 ± 3
Sawdust treated with whey UF permeate	226 ± 2	240 and 325	30.0 ± 0
Sawdust treated with AMPUL	211 ± 3	247.5 and 328	21.0 ± 3
Sawdust treated with lactose	230 ± 3	253, 313 and 360	16.0 ± 0

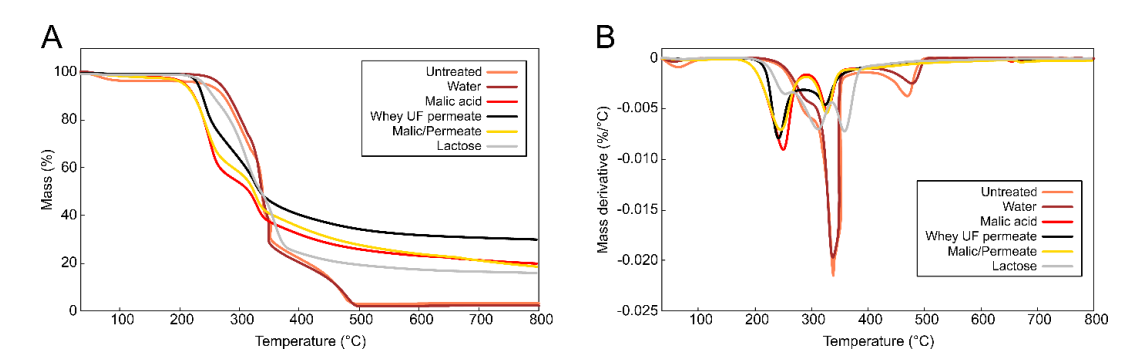


Fig. 15. Comparison of the thermal stability with A) TGA and B) DTG of untreated sawdust, sawdust treated with water, malic acid, whey ultrafiltration permeate, malic-permeate solution (AMPUL), or lactose under a nitrogen atmosphere

Sorption behavior of untreated trembling aspen sawdust and trembling aspen sawdust treated with different solutions

Figure 16 shows the sorption isotherm curves of the untreated and treated samples, and the corresponding moisture content at 95% RH is presented in Table 8. In the 0 to 30% RH range, the moisture content (MC) of untreated trembling aspen sawdust increased logarithmically, indicating that water molecules initially entered the wood through "monolayer adsorption" (Luo *et al.* 2024). Subsequently, water molecules aggregated and adsorbed directly in the form of "multimolecular adsorption" *via* hydrogen bonds.

Table 8. Moisture Content of Untreated Sawdust and Sawdust Treated with Different Solutions

Sample	Moisture Content ¹ (%)
Untreated sawdust	20 ± 0
Sawdust treated with water	20 ± 1
Sawdust treated with malic acid	14 ± 0
Sawdust treated with whey UF permeate	34 ± 4
Sawdust treated with AMPUL	13 ± 1
Sawdust treated with lactose	19 ± 0

¹Determined at 95% relative humidity

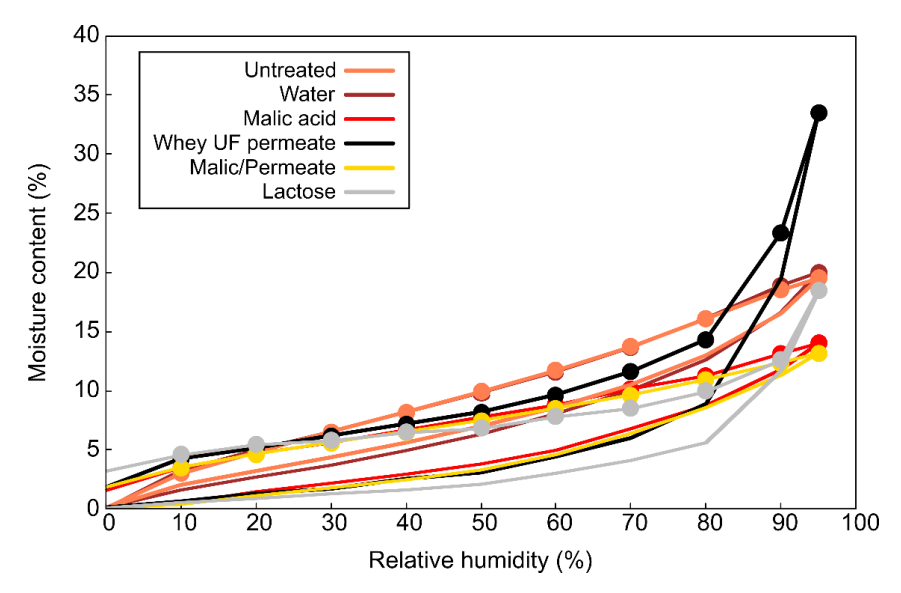


Fig. 16. Comparison of the sorption isotherm of the untreated sawdust and sawdust treated with different solutions. Lines with and without symbols indicate desorption and adsorption curves, respectively

When the RH exceeded 60%, the MC increased sharply, resembling an exponential curve. Therefore, the untreated trembling aspen sawdust sorption isotherm exhibited a sigmoid shape, characteristic of a type II sorption isotherm (Niemz et al. 2023; Hill et al. 2024). The sorption isotherms for trembling aspen sawdust treated with different solutions were similar to that of untreated sawdust. However, the MC of trembling aspen sawdust treated with malic acid and AMPUL was lower across the entire hygroscopic range. This reduction in MC is attributed to the occupation of water adsorption sites by the reaction of malic acid with the wood cell wall in the case of the treatment with malic acid and products formed between malic acid, and whey ultrafiltration permeate within the wood structure for the treatment with AMPUL. For the sample treated with water, there was no significant difference compared to the untreated sample, suggesting that the curing temperature did not affect wood hygroscopicity. The observed changes in samples treated with malic acid and AMPUL were due to the treatment itself, independent of curing temperature. For the sample treated with whey ultrafiltration permeate alone, water adsorption was lower than that of the untreated sample at lower RH values. However, when RH exceeded 80%, the MC increased exponentially and surpassed that of the untreated sample. This behavior is likely due to the products formed during curing of the whey ultrafiltration permeate, which occupied the sites for the "monolayer adsorption" at low RH. At high RH values, hydrogen bonds facilitated this exponential water adsorption, with the products being rich in oxygen and hydrogen, enhancing hydrogen bonding with water molecules. The hygroscopic behavior of trembling aspen sawdust treated with lactose was similar to that of sawdust treated with whey ultrafiltration permeate. However, the MC was higher for the sample treated with whey ultrafiltration permeate. This difference is likely due to its ash content, which would contribute to the moisture uptake.

Hysteresis curves describe the response of the wood cell to the ingress and egress of water molecules under conditions of adsorption and desorption (Anwar Uyup *et al.* 2021; Niemz *et al.* 2023); specifically, the moisture content reached by desorption is higher than that reached by absorption at the same RH and temperature. Figure 17 compares the hysteresis of untreated trembling aspen sawdust with those of trembling aspen sawdust

treated with different solutions. Overall, the hysteresis value for all samples exhibited an increasing and then decreasing trend as the RH increased. As observed in the sorption isotherm curves, the hysteresis of the water-treated sample was similar to that of the untreated sample (Fig. 17 - Water). For samples treated with malic acid and AMPUL, their hysteresis curves were higher than that of the untreated sample at RH range 0 to 70% and then became lower. This implies that at higher RH, the adsorbed water had weaker interactions in the treated samples compared to the untreated sample. At low RH, due to cell wall modification, the water adsorbed during the adsorption cycle was trapped in the cell wall, and the same RH during the desorption cycle was insufficient to remove it from the cell wall. For the whey ultrafiltration permeate-treated sample (Fig. 17 – Whey ultrafiltration permeate), the hysteresis curve remained higher than that of the untreated sample across the entire RH range. This behavior is likely due to the formation of oxygen-and hydrogen-rich products during the heating of whey ultrafiltration permeate, which resulted in strong interaction with water molecules even at high RH values. For the sample treated with lactose, the same trend was observed in malic and AMPUL treatments.

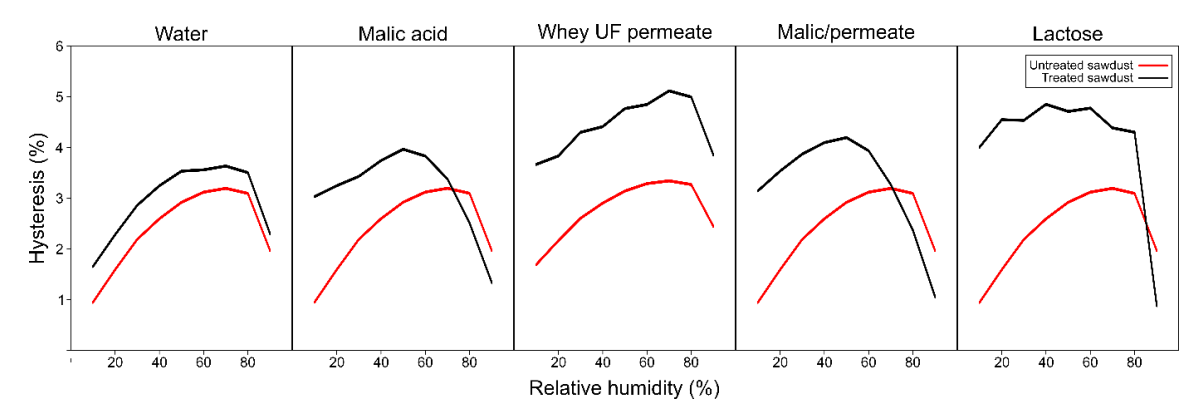


Fig. 17. Comparison of the sorption isotherms of the untreated sawdust and sawdust treated with different solutions

CONCLUSIONS

- 1. Whey ultrafiltration permeate was found to undergo the Maillard reaction when heated to 160 °C. The lactose in whey ultrafiltration permeate caramelized in an acidic medium at this temperature. In the presence of organic acids such as citric, malic, and succinic acids, the lactose in whey ultrafiltration reacted with these acids through a polycondensation reaction when heated at 160 °C. Side reactions such as caramelization and the Maillard reaction may also occur during this process.
- 2. When trembling aspen sawdust was impregnated with a mixture of malic acid and whey ultrafiltration permeate, a significant decrease in moisture uptake was observed compared to the untreated samples. Additionally, the treated samples showed higher thermal stability compared to the untreated ones, and other treated samples (except the one including whey ultrafiltration permeate), meaning the positive effect of ash contained in whey ultrafiltration permeate. The reference samples (impregnated with water alone) did not show significant changes compared to the untreated samples, indicating that the effectiveness of the treatment was not dependent on the curing temperature.

3. As previous research has shown, reduced moisture absorption in wood suggests increased dimensional stability and resistance to microorganisms. These aspects are currently under investigation. This study presents a novel method for adding value to whey ultrafiltration permeate, a by-product whose production has steadily increased in North America in recent years.

ACKNOWLEDGMENTS

The authors would like to thank Fonds de Recherche du Québec - Nature et Technologie and Natural Sciences and Engineering Research Council of Canada for the financial support of this project through the NOVA program (ALLRP 571482 – 21 and 2023-NOVA-315224). The authors are grateful to Yves Bédard and Luc Germain for their support during the characterization and preparation of the samples. While preparing this work, the authors used an artificial intelligence tool to review the English quality of the manuscript.

REFERENCES CITED

- Ames, J. M. (1998). "Applications of the Maillard reaction in the food industry," *Food Chemistry* 62(4), 431-439. DOI: 10.1016/S0308-8146(98)00078-8
- Anwar Uyup, M. K., Sahari, S. H., Jalaludin, Z., Husain, H., Lee, S. H., and Yusoh, A. S. (2021). "Water vapour sorption behaviour and physico-mechanical properties of methyl methacrylate (MMA)- and MMA–styrene-modified batai (*Paraserianthes falcataria*) wood," *Holzforschung* 75(5), 444-451. DOI: 10.1515/hf-2020-0005
- Berube, M.-A., Schorr, D., Ball, R. J., Landry, V., and Blanchet, P. (2018). "Determination of *in situ* esterification parameters of citric acid-glycerol based polymers for wood impregnation," *Journal of Polymers and the Environment* 26(3), 970-979. DOI: 10.1007/s10924-017-1011-8
- Buera, M. D. P., Chirife, J., Resnik, S. L., and Lozano, R. D. (1987). "Nonenzymatic browning in liquid model systems of high water activity: Kinetics of color changes due to caramelization of various single sugars," *Journal of Food Science* 52(4), 1059-1062. DOI: 10.1111/j.1365-2621.1987.tb14275.x
- Cadieux-Lynch, R., Leroux, E., Hermann, A., Pellerin, S., Keralta, A., Blouin, M., Larouche, J., Profili, J., Chamberland, J., and Landry, V. (2024). "From waste to building material: How whey ultrafiltration permeate can increase wood stability," *Journal of Materials Research and Technology* S223878542400228X. DOI: 10.1016/j.jmrt.2024.01.228
- Chamberland, J., Bouyer, A., Benoit, S., Provault, C., Bérubé, A., Doyen, A., and Pouliot, Y. (2020). "Efficiency assessment of water reclamation processes in milk protein concentrate manufacturing plants: A predictive analysis," *Journal of Food Engineering* 272, article 109811. DOI: 10.1016/j.jfoodeng.2019.109811
- Earl, W. L., and Parrish, F. W. (1983). "A cross-polarization—magic-angle sample spinning NMR study of several crystal forms of lactose," *Carbohydrate Research* 115, 23-32. DOI: 10.1016/0008-6215(83)88131-2
- Elrhayam, Y., and El Bachiri, A. (2024). "Study of the effect of heat temperature on the chemical changes and hygroscopicity of eucalyptus wood by FT-IR and prediction of

- mechanical properties by the MLR regression method," *Spectrochimica Acta Part A: Molecular and Biomolecular Spectroscopy* 124576. DOI: 10.1016/j.saa.2024.124576
- Grosse, C., Noël, M., Thévenon, M. F., Rautkari, L., and Gérardin, P. (2018). "Influence of water and humidity on wood modification with lactic acid," *Journal of Renewable Materials*, 6(3), 259-269. DOI: 10.7569/JRM.2017.634176
- Hagen, M., Hereid, J., Delichatsios, M. A., Zhang, J., and Bakirtzis, D. (2009). "Flammability assessment of fire-retarded Nordic Spruce wood using thermogravimetric analyses and cone calorimetry," *Fire Safety Journal* 44(8), 1053-1066. DOI: 10.1016/j.firesaf.2009.07.004
- Halpern, J. M., Urbanski, R., Weinstock, A. K., Iwig, D. F., Mathers, R. T., and Von Recum, H. A. (2014). "A biodegradable thermoset polymer made by esterification of citric acid and glycerol: Biodegradable thermoset polymer," *Journal of Biomedical Materials Research Part A* 102(5), 1467-1477. DOI: 10.1002/jbm.a.34821
- Hill, C. A. S. (2002). "How does the chemical modification of wood provide protection against decay fungi?," in: *Proceedings of the COST E22 Meeting*.
- Hill, C. A. S. (2006). *Wood Modification: Chemical, Thermal and Other Processes*, John Wiley & Sons, Hoboken, NJ, USA.
- Hill, C. A. S. (2011). "Wood modification: An update," *BioResources* 6(2), 918-919. DOI: 10.15376/biores.6.2.918-919
- Hill, C. A. S., Altgen, M., Penttilä, P., and Rautkari, L. (2024). "Review: Interaction of water vapour with wood and other hygro-responsive materials," *Journal of Materials Science*. DOI: 10.1007/s10853-024-09636-y
- Hill, C. A. S., Forster, S. C., Farahani, M. R. M., Hale, M. D. C., Ormondroyd, G. A., and Williams, G. R. (2005). "An investigation of cell wall micropore blocking as a possible mechanism for the decay resistance of anhydride modified wood," *International Biodeterioration & Biodegradation* 55(1), 69-76. DOI: 10.1016/j.ibiod.2004.07.003
- Kroh, L. W. (1994). "Caramelisation in food and beverages," *Food Chemistry* 51(4), 373-379. DOI: 10.1016/0308-8146(94)90188-0
- Kurkowiak, K., Hentges, D., Dumarçay, S., Gérardin, P., and Militz, H. (2023).
 "Understanding the mode of action of sorbitol and citric acid (SorCA) in wood,"
 Wood Material Science & Engineering 18(1), 67-75. DOI:
 10.1080/17480272.2022.2125340
- Luo, C., Hou, S., Mu, J., and Qi, C. (2024). "How does phosphoric acid affect the hygroscopicity and chemical components of poplar thermally modified at low temperatures?," *Wood Science and Technology*. DOI: 10.1007/s00226-024-01543-4
- Nielsen, S. D., Knudsen, L. J., Bækgaard, L. T., Rauh, V., and Larsen, L. B. (2022). "Influence of lactose on the Maillard reaction and dehydroalanine-mediated protein cross-linking in casein and whey," *Foods* 11(7), article 897. DOI: 10.3390/foods11070897
- Niemz, P., Teischinger, A., and Sandberg, D. (eds.). (2023). *Handbook of Wood Science and Technology*, Springer International Publishing, Cham. DOI: 10.1007/978-3-030-81315-4
- Popescu, C.-M., Hill, C. A. S., Curling, S., Ormondroyd, G., and Xie, Y. (2014). "The water vapour sorption behaviour of acetylated birch wood: How acetylation affects the sorption isotherm and accessible hydroxyl content," *Journal of Materials Science* 49, 2362-2371. DOI: 10.1007/s10853-013-7937-x
- Sengar, G., and Sharma, H. K. (2014). "Food caramels: A review," Journal of Food

- Science and Technology 51(9), 1686-1696. DOI: 10.1007/s13197-012-0633-z
- Shen, H., Shan, H., and Liu, L. (2020). "Evolution process and controlled synthesis of humins with 5-hydroxymethylfurfural (HMF) as model molecule," *ChemSusChem* 13(3), 513-519. DOI: 10.1002/cssc.201902799
- Shi, J., Lu, Y., Zhang, Y., Cai, L., and Shi, S. Q. (2018). "Effect of thermal treatment with water, H2SO4 and NaOH aqueous solution on color, cell wall and chemical structure of poplar wood," *Scientific Reports* 8(1), article 17735. DOI: 10.1038/s41598-018-36086-9
- Srebotnik, E., Messner, K., and Foisner, R. (1988). "Penetrability of white rot-degraded pine wood by the lignin peroxidase of *Phanerochaete chrysosporium*," *Applied and Environmental Microbiology* 54(11), 2608-2614. DOI: 10.1128/aem.54.11.2608-2614.1988
- Sun, S., Zhao, Z., and Umemura, K. (2019). "Further exploration of sucrose-citric acid adhesive: Synthesis and application on plywood," *Polymers* 11(11), article 1875. DOI: 10.3390/polym11111875
- Sundqvist, B., and Morén, T. (2002). "The influence of wood polymers and extractives on wood colour induced by hydrothermal treatment," *Holz als Roh- und Werkstoff* 60(5), 375-376. DOI: 10.1007/s00107-002-0320-2
- Xu, Z., Yang, Y., Yan, P., Xia, Z., Liu, X., and Zhang, Z. C. (2020). "Mechanistic understanding of humin formation in the conversion of glucose and fructose to 5-hydroxymethylfurfural in [BMIM]Cl ionic liquid," *RSC Advances* 10(57), 34732-34737. DOI: 10.1039/D0RA05641C
- Yaylayan, V. A. (1997). "Classification of the Maillard reaction: A conceptual approach," Trends in Food Science & Technology 8(1), 13-18. DOI: 10.1016/S0924-2244(96)20013-5
- Ye, X., Hu, T., and Liu, L. (2024). "Evolution process of humins derived from xylose," *ACS Sustainable Chemistry & Engineering*, acssuschemeng.4c02535. DOI: 10.1021/acssuschemeng.4c02535
- Zhang, M., Yang, H., Liu, Y., Sun, X., Zhang, D., and Xue, D. (2012). "First identification of primary nanoparticles in the aggregation of HMF," *Nanoscale Research Letters* 7(1), article 38. DOI: 10.1186/1556-276X-7-38
- Zhao, Sakai, Wu, Chen, Zhu, Huang, Sun, Zhang, Umemura, and Yong. (2019). "Further exploration of sucrose-citric acid adhesive: Investigation of optimal hot-pressing conditions for plywood and curing behavior," *Polymers* 11(12), article 1996. DOI: 10.3390/polym11121996

Article submitted: December 3, 2024; Peer review completed: January 4, 2025; Revised version received: April 15, 2025; Accepted: May 2, 2025; Published: May 29, 2025. DOI: 10.15376/biores.20.3.5843-5869

APPENDIX

Supplementary Information

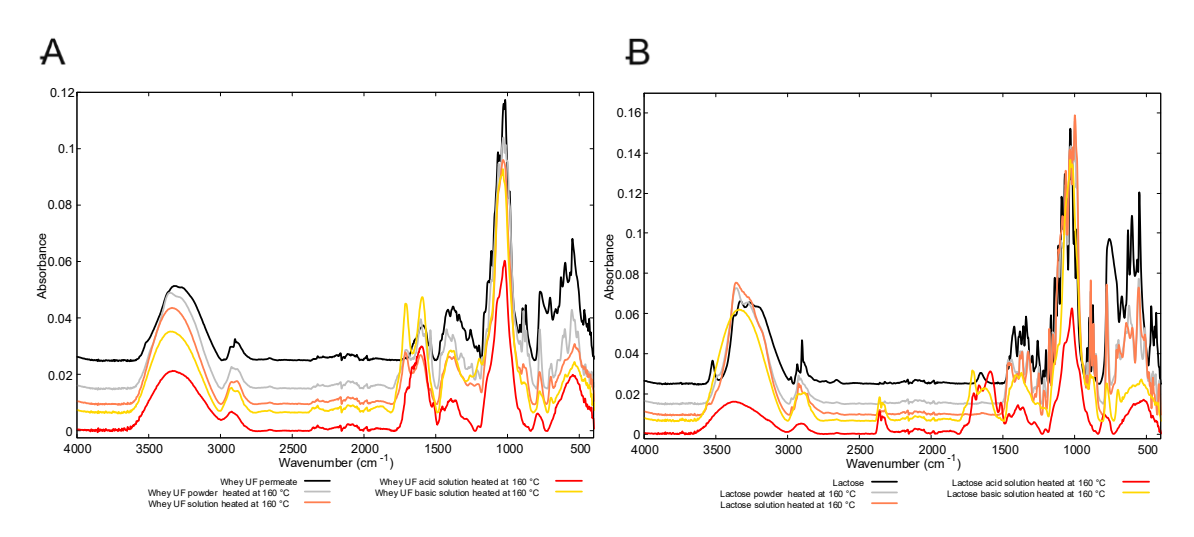


Fig S1. Full FTIR spectra of products from the thermal degradation of whey ultrafiltration permeate (a) and lactose (b)